

# Evaluating the use of outputs from comprehensive meteorological models in air quality modeling applications

Vlad Isakov<sup>a,\*</sup>, Akula Venkatram<sup>b</sup>, Jawad S. Touma<sup>a</sup>, Darko Koračin<sup>c</sup>,  
Tanya L. Otte<sup>a</sup>

<sup>a</sup>*NOAA/Atmospheric Sciences Modeling Division, Research Triangle Park, NC 27711, USA*

<sup>b</sup>*University of California, Riverside, CA 92521, USA*

<sup>c</sup>*Desert Research Institute, 2215 Raggio Parkway, Reno, NV 89512, USA*

Received 25 May 2006; received in revised form 15 October 2006; accepted 17 October 2006

---

## Abstract

Currently used dispersion models, such as the AMS/EPA Regulatory Model (AERMOD), process routinely available meteorological observations to construct model inputs. Thus, model estimates of concentrations depend on the availability and quality of meteorological observations, as well as the specification of surface characteristics at the observing site. We can be less reliant on these meteorological observations by using outputs from prognostic models, which are routinely run by the National Oceanic and Atmospheric Administration (NOAA). The forecast fields are available daily over a grid system that covers all of the United States. These model outputs can be readily accessed and used for dispersion applications to construct model inputs with little processing. This study examines the usefulness of these outputs through the relative performance of a dispersion model that has input requirements similar to those of AERMOD. The dispersion model was used to simulate observed tracer concentrations from a Tracer Field Study conducted in Wilmington, California in 2004 using four different sources of inputs: (1) onsite measurements; (2) National Weather Service measurements from a nearby airport; (3) readily available forecast model outputs from the Eta Model; and (4) readily available and more spatially resolved forecast model outputs from the MM5 prognostic model. The comparison of the results from these simulations indicate that comprehensive models, such as MM5 and Eta, have the potential of providing adequate meteorological inputs for currently used short-range dispersion models such as AERMOD.

© 2006 Elsevier Ltd. All rights reserved.

*Keywords:* Prognostic meteorological models; Dispersion modeling; Model evaluation; Tracer experiment; Thermal internal boundary layer

---

## 1. Introduction

Meteorological data are critical inputs in dispersion models such as AERMOD (Cimorelli et al.,

2005), which was introduced recently by the US Environmental Protection Agency (EPA) as a replacement for Industrial Source Complex (ISC) model for estimating the air quality impact of sources for source–receptor distances of kilometers. AERMOD is designed to use vertical profiles of wind speed and turbulence measured at the site

---

\*Corresponding author. Tel.: +1 919 541 2494.

E-mail address: [Isakov.Vlad@epa.gov](mailto:Isakov.Vlad@epa.gov) (V. Isakov).

where the model is applied. Currently AERMOD can accept the following turbulence measurements: standard deviation of the horizontal wind component,  $\sigma_{\theta}$ , and standard deviation of the vertical wind component,  $\sigma_w$ . There are future plans to include other turbulence parameters. Such meteorological observations are usually not available at most sites of interest, and insisting on site-specific measurements is not practical. Thus, AERMOD uses a processor to construct inputs from routinely available National Weather Service (NWS) surface and upper air data from nearby locations. Using NWS observations can pose problems because observation sites can be located tens or even hundreds of kilometers from the location at which AERMOD is being applied. Also, upper air meteorological data needed to estimate mixing heights are usually not collocated with the surface observations. Thus, these data are often not representative of the application site. Furthermore, because the data have to be quality controlled and archived by the National Climatic Data Center (NCDC), they might not be available for months after they are collected.

One possible way for solving this problem with meteorological inputs is to use comprehensive meteorological models to provide estimates of the boundary layer variables required by AERMOD at the site of interest. Because these models have a long history of use in regional air quality models such as the Regional Acid Deposition Model (Chang et al., 1987) and the EPA's Community Multiscale Air Quality (CMAQ) modeling system (Byun and Ching, 1999; Byun and Schere, 2006) their accuracy has improved over the past decade as process parameterizations have been improved by the growing user community. There is an extensive history of coupling numerical weather prediction models and dispersion models (e.g. Yamada et al., 1992; Draxler and Hess, 1998; Draxler, 2003). Outputs from prognostic models run by the National Oceanic and Atmospheric Administration (NOAA) are available in near-real-time over a 12 km grid system that covers the United States. Thus, a model user has ready access to the most recent meteorological data, which can be used in air quality simulations with little further processing. In the future, it should be possible to convert these data to the formats needed for air quality dispersion models at nominal cost. In addition, the formats for the meteorological data from comprehensive models will become standardized as EPA moves to a

“one-atmosphere” modeling approach involving national to local scales air quality assessments (Touma et al., 2006).

This paper examines whether gridded outputs from comprehensive meteorological models can be used to construct meteorological inputs for dispersion models such as AERMOD. These outputs correspond to forecast data from two comprehensive meteorological models: the National Centers for Environmental Prediction's (NCEP's) North American Mesoscale (NAM) Model, i.e., the Eta Model (Black, 1994; Rogers et al., 1996), and the fifth-generation Penn State/National Center for Atmospheric Research Mesoscale Model (MM5) (Grell et al., 1995). The Eta model output fields used here are specifically processed for air quality forecasting system (Otte et al., 2005) and are generated with 12-km horizontal grid spacing. Although these models are commonly used in NWS practice (Cheng and Steenburgh, 2005), it is important to assess the ability of operational models to be used as drivers for air pollution modeling and forecasting. Some of the studies demonstrate the limitations of the Eta model in accurately predicting winds in the boundary layer and suggest that for accurate predictions, the horizontal resolution should be about 5 km in complex terrain (e.g., Cairns and Corey, 2003). The version of MM5 used here provides forecasts for Southern California at 3 km horizontal grid spacing (DRI, 2005).

The value of these meteorological model outputs for air quality modeling is evaluated by first comparing them with measurements made onsite, and then using them as inputs to a dispersion model and comparing its performance to those based on the following inputs: (1) onsite measurements relevant to AERMOD, and (2) AERMOD inputs derived from the nearest National Weather Service (NWS) stations. The meteorological inputs correspond to a field study conducted in Wilmington, California, in 2004, which is described next.

## 2. Wilmington field study

The Wilmington field experiment was conducted by the University of California, Riverside (UCR) in the vicinity of the Harbor Generating Station of the City of Los Angeles's Department of Water and Power (LADWP), located in Wilmington, California (Yuan et al., 2006). The objective of the

study was to collect data that could be used to formulate and evaluate dispersion models applicable to both surface as well as elevated sources located in shoreline urban areas.

Wilmington is a community of about 53,000 people located next to the Port of Los Angeles. It is surrounded by numerous small industries, transportation corridors, and port businesses, which are located to the south of residential areas. Fig. 1 displays the map of Wilmington. The residential areas, consisting mostly of one story buildings of about 4 m high, are located downwind of the release point inside the LADWP site during the dominant southeasterly flows. The building density is relatively low, suggesting small flow wake interference.

### 2.1. Tracer concentration measurements

Tracer studies were conducted on 8 days during the period 26 August to 10 September 2004. Each study day involved release of the inert tracer gas, sulfur hexafluoride ( $\text{SF}_6$ ), over periods lasting from

2 to 6 h. During the first 6 days, diluted  $\text{SF}_6$  was released at the base of a stack of the Los Angeles Department of Water & Power (LADWP) generating station, which is located  $\sim 0.8$  km from the ocean, adjacent to the Port of Los Angeles. During the last two study days, diluted  $\text{SF}_6$  was released near the surface in an open area inside the generating station. The released tracer was sampled along five arcs. Three of the arcs were located approximately 1000, 3000, and 5000 m from the release point. The fourth and fifth set of samplers was placed along radial distances ranging between 100 and 400 m from the source. Eighteen samplers were placed at  $6^\circ$  spacing on the 1000 and 3000 m arcs, while eight and eleven samplers were placed approximately  $5^\circ$  apart on the 100 and 400 m arcs, respectively. There were 17 samplers on the 5000 m arc, with two additional samplers collocated at the two sites for quality control purposes. The locations of these samplers are also shown in Fig. 1. Measurements on a mobile monitoring van using a real-time continuous monitor were used to supplement the stationary samples.

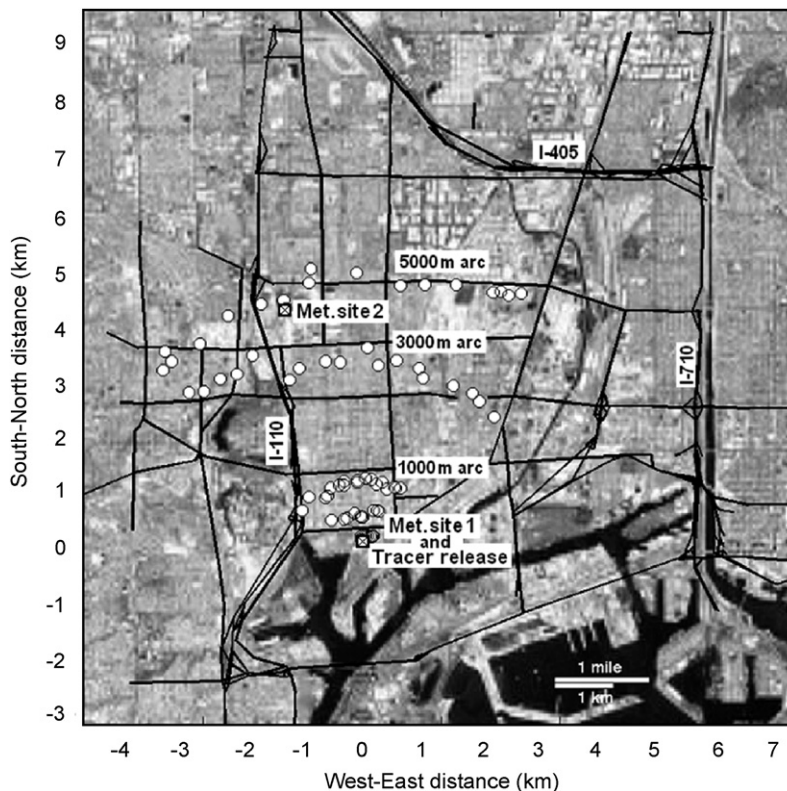


Fig. 1. Map of study area and equipment locations.

## 2.2. Meteorological measurements

The location of the instruments is shown in Fig. 1. At “Met. Site 1”, a sonic anemometer with sensors placed at a height of 3 m was used to measure surface winds. Winds aloft (up to approximately 600 m) were measured using an acoustic sounder. At “Met. Site 2”, the downwind monitoring site, a second sonic anemometer at a height of 3 m, an acoustic sounder, and a remote sensing microwave temperature sounder, used to determine the vertical temperature profile from the surface to 600 m AGL, were placed in an open area at Los Angeles County Sanitation District’s Joint Water Pollution Control Plant (JWPCP), located ~4 km downwind of the source. The three components of velocity and temperature were sampled at 10 Hz using sonic anemometers. These measurements were used to derive 1 h averaged mean winds and temperatures, standard deviations of the turbulent velocity fluctuations, and turbulent momentum and heat fluxes. Winds and turbulence above the urban canopy were measured using the acoustic sounder that took measurements from 15 m up to 200 m at a resolution of 5 m, and the full-sized sounder which provided information up to heights of 600 m above-ground level. The meteorological measurements provided vertical profiles of wind speed, turbulence, and temperature.

Approximately 1 month of data consisting of 10 Hz velocities and temperatures covering a wide variety of meteorological conditions was collected. The experiments were conducted during daytime hours when the whole area of the field study was dominated by south or southeast onshore flows. The surface boundary layer was convective for most of the experiments, except for the 24th trial conducted on 9/3/2004 at 7:00 a.m. local standard time (LST). The height range of valid data from the acoustic sounder was ~15–100 m. The winds and the turbulent velocity statistics varied little above 50 m. Because the internal boundary layer (discussed later) that limited vertical dispersion rarely exceeded 200 m, the measured values of winds and turbulence at 50 m were used to represent the boundary layer variables used in the dispersion model.

The second set of AERMOD inputs was derived from meteorological data from the National Weather Service (NWS) station at the Long Beach airport, approximately 10 km northeast of the site and in the same meteorological regime as

the site. These data were processed for use in AERMOD.

The following sections provide brief descriptions of the outputs from the meteorological models that were used to construct inputs for dispersion models, such as AERMOD.

## 2.3. Meteorological model outputs from Eta Model

The National Center for Environmental Prediction’s (NCEP’s) North American Mesoscale (NAM) Model, i.e., the Eta Model (Black, 1994; Rogers et al., 1996) for the time periods in this study, generates multi-day gridded meteorological forecasts for North America four times daily. The outputs from the NAM Model are used in the national air quality forecasting (AQF) system, which couples the NAM Model and CMAQ. The NAM–CMAQ forecasting system currently issues twice-daily 48-h gridded ozone predictions for the United States (Otte et al., 2005), and requires hourly input meteorological data. Currently, the NAM Model fields are used for the AQF with a 12-km horizontal grid spacing nationwide on a Lambert conformal map projection. In the NAM fields that are used in this study, forecast output from the 60 step-mountain eta layers on the Eta Model’s full horizontal domain are interpolated to 22 hydrostatic sigma-pressure layers that are used by CMAQ. There are approximately 12 layers below 2 km AGL, and the lowest layer thickness is about 39 m. As necessary, the NAM Model postprocessor diagnoses additional forecast variables for the AQF system, and some of these fields are required inputs for AERMOD. In this study, we use meteorological data generated by the NAM Model, i.e., the Eta Model, for the AQF system for one 12-km cell corresponding to the area encompassed by the tracer experiment in Wilmington, California, during August and September, 2004. It should be noted that the NAM Model output fields that are used in this study are specific to the AQF system and are not disseminated by NCEP.

## 2.4. Meteorological model outputs from MM5 modeling system

The MM5 real-time forecasting system provided by the Desert Research Institute (DRI, 2005) is updated twice daily at 0530 and 1730 UTC for the three model domains. In this study, the MM5 forecasts for the 3-km domain corresponding to the

area of the Wilmington tracer experiment are used. Mesoscale Model 5 is used worldwide and was developed jointly by Pennsylvania State University and the National Center for Atmospheric Research in Boulder, Colorado. Details of the

model structure are described by Grell et al. (1995). Mesoscale Model 5 has been used in a variety of research and application studies focused on atmospheric dynamics, cloudiness, and fog along the California coast (Koraćin and Dorman, 2001; Koraćin et al., 2004, 2005), among others. To account for synoptic processes and also to resolve the characteristics of the mesoscale processes, coarse and nested grids were set up to cover a large portion of the US West Coast from southern Oregon to Baja California. A coarse grid ( $90 \times 90 \times 35$  grid points) with 27 km horizontal grid spacing is set up to cover most of the southwestern United States. The inner domain ( $121 \times 127 \times 35$  grid points) with a horizontal grid spacing of 9 km is nested within the coarse domain and covers all California land and coastal waters as well as all of Nevada as shown in Fig. 2. The innermost grid ( $100 \times 82 \times 35$  grid points) with the horizontal grid spacing of 3 km focuses on Southern California. Each model domain consists of 36 full-sigma levels. The first vertical level is at about 10 m height and there are 9 levels in the lowest kilometer. Horizontal wind components and thermodynamic variables are computed on half-sigma levels, while vertical velocity is computed on full-sigma levels. Topography input was extracted from the 30''-resolution global terrain and land-use files. The main physics

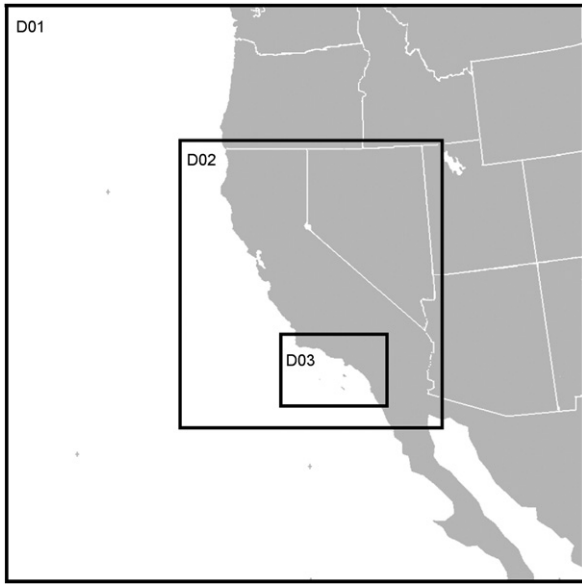


Fig. 2. Geographical setup of model domains for the operational version of MM5.

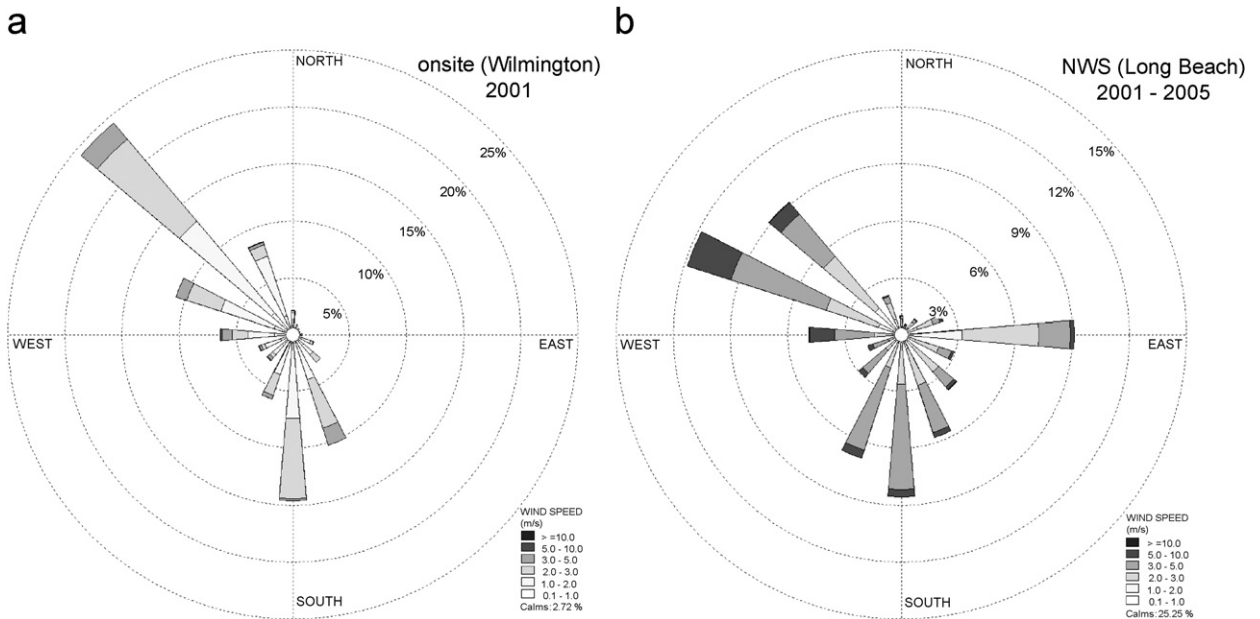


Fig. 3. Wind roses of observed winds at KLGB NWS station for all hours from 26 August to 10 September 2004 (a), and only for hours of tracer experiments (b).

options included simple ice microphysics; the Mellor-Yamada Level 2.5 “Eta” parameterization (Janjic, 1994) to compute turbulence fluxes in the

planetary boundary layer (PBL); and a multi-layer soil model for land surface temperature prediction. First guess fields and lateral boundary conditions

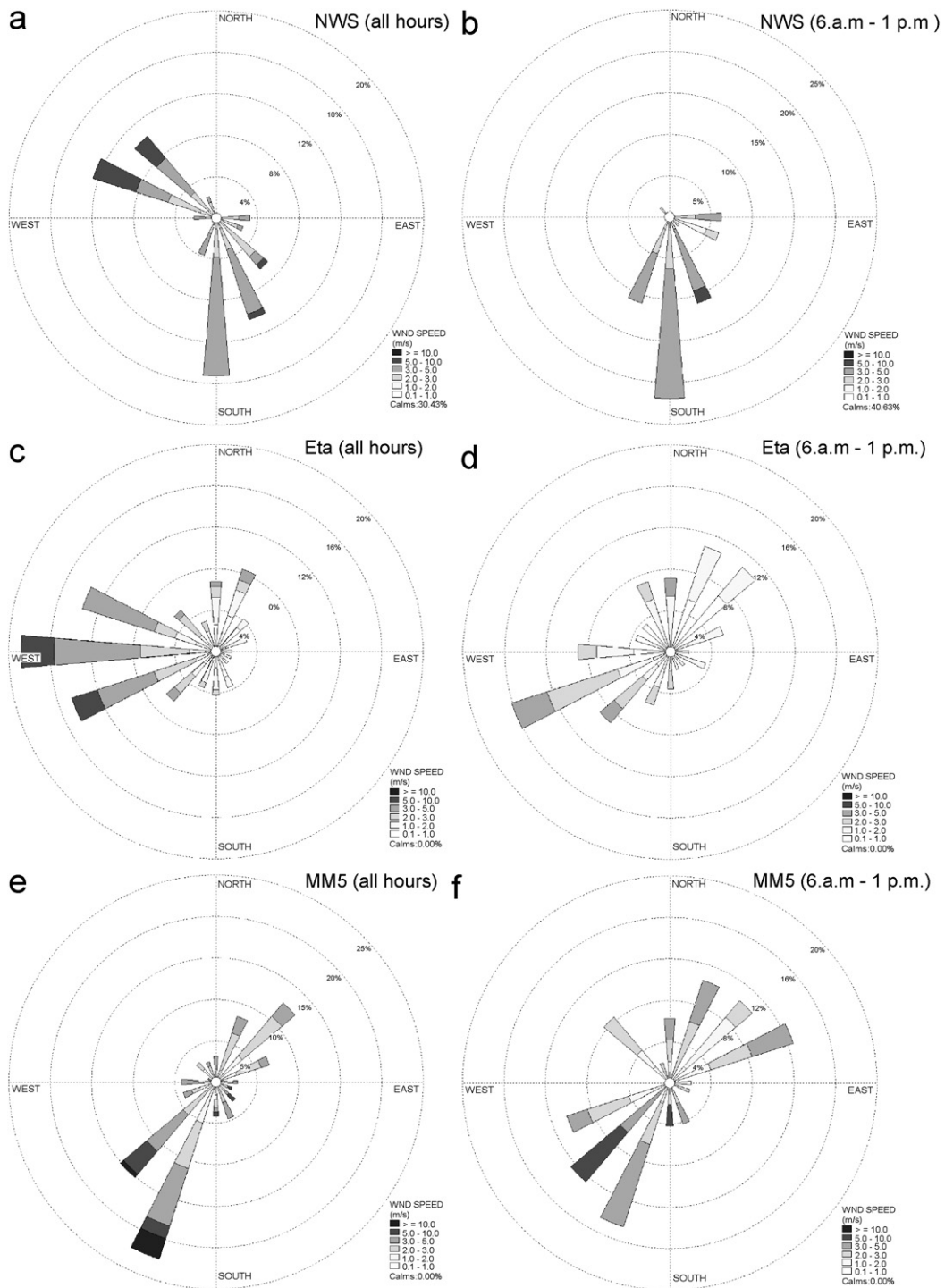


Fig. 4. Wind roses of simulated winds derived from NWS observations (a), from the Eta Model (c), and from MM5 (e) for all hours from August 26th to September 10th; and only during hours of tracer experiments (b, d, f).

for the coarse grid for every 12 h are obtained from the Eta model simulation. Synoptic information includes virtual temperature, geopotential height, horizontal wind components, and relative humidity with a horizontal resolution of 40 km. These first-guess fields were horizontally interpolated onto the model grid by a two-dimensional, 16-point overlapping parabolic fit. In the second step of the preprocessing the first guess fields were refined using observations. Similarly, the first-guess sea-surface temperature (SST) field was extracted from the US Navy's daily values (with a horizontal resolution of  $2.5^\circ$  in both latitudinal and longitudinal directions), updated with buoy and coastal station data, and interpolated onto the model grid using a bilinear interpolation method. Time steps on the coarse and nested grids were 81, 27, and 9 s, respectively.

The next section provides a preliminary comparison of the forecasts from the two models with observations from the Long Beach NWS site.

### 3. Evaluation of results from prognostic meteorological models

Meteorological conditions in Wilmington, CA are influenced by the dominant northwesterly flow along the coast as indicated in Fig. 3a, and also by southerly flow due to the ocean breeze during the day. The samplers located on the three arcs, shown in Fig. 1, measure tracer concentrations when the flow is from the south.

The nearest NWS station at the Long Beach airport is located approximately 10 km northeast of the site. Wind roses of observed winds from the Long Beach airport for the 5-year period are shown in Fig. 3b.

Fig. 4 shows wind roses of simulated winds derived from NWS observations, and simulated by the Eta and MM5 meteorological models during the hours the tracer experiments were conducted. The NWS observations indicate that surface flows are predominantly from the south, south-east, and from the northwest. The southerly component is related to the sea breeze that occurs during the late morning and early hours; the 6 am–1 pm wind rose in the right panel shows this feature.

The predicted wind flows from the 12-km Eta Model indicate an incorrect dominant westerly flow with lobes in the NW and the SW directions. The observed southerly component associated with the sea breeze is completely absent in the wind rose. The wind rose associated with the period 6 am–1 pm

shows a slight shift to the WSW dominance, but the large southerly sea breeze component is missing.

The MM5 model with a 3 km spatial resolution does much better in capturing the effect of the sea breeze. However, it misses the NW lobe for all hours. The 6 am–1 pm wind rose also shows SW wind flows but misses the dominant southerly flow. Also, the wind rose shows North Easterly components that are absent in the NWS data.

Routine applications of the Eta Model and MM5 do not provide the surface micro-meteorological inputs or the PBL heights required by dispersion models. However, the models predict fields of turbulent kinetic energy (TKE), which can be related to the standard deviations of the turbulent velocities that govern dispersion in the PBL. This is described in the next section.

### 4. Meteorological inputs for dispersion models

The turbulent velocities required by the dispersion model are not direct outputs of Eta and MM5, although in principle these models could be modified to produce them. For this application, we derived these velocities from the turbulent kinetic energy given by

$$\text{TKE} = \frac{1}{2}(\sigma_u^2 + \sigma_v^2 + \sigma_w^2). \quad (1)$$

The TKE was distributed among its three components using ratios corresponding to neutral conditions (Hanna and Britter, 2001)

$$\begin{aligned} \sigma_w &= 0.55k, \\ \sigma_v &= 0.81k, \\ \sigma_u &= 1.02k, \end{aligned} \quad (2)$$

where  $k = (\text{TKE})^{1/2}$ . Because the TKE reflects the buoyancy production of turbulence included in the comprehensive meteorological models, the turbulent velocities computed from Eq. (2) account for stability effects.

We conducted this study with a dispersion model that is similar to AERMOD in structure and input requirements. We did not use AERMOD directly to avoid dealing with the cumbersome mechanics of running the AERMOD code. The mean winds and the turbulent velocities (Eq. (2)) from MM5 and Eta constituted inputs to this dispersion model. In principle, we could have used AERMOD's meteorological processor, AERMET, to construct the required micrometeorological inputs treating the

mean wind and temperature estimates from MM5 and NAM as NWS measurements. Although this is an option, we wanted to treat the comprehensive models as real systems in which mean and turbulence variables can be accessed without making expensive measurements.

It turns out that for near surface releases (Yuan et al., 2006), the centerline ground-level concentrations are inversely proportional to the dilution velocity given by

$$u_{\text{dil}} = \frac{\sigma_w \sigma_v}{U}, \tag{3}$$

where all the variables correspond to values averaged over the plume depth.

The vertical spread of the plume is limited by the height of the internal boundary layer that forms when the stable air from the ocean flows onto

warmer land. The height of this internal boundary layer,  $H$ , was inferred from observations of ground-level concentrations (Yuan et al., 2006), and was empirically given by,

$$H = 8 \frac{\sigma_w}{N}, \tag{4}$$

at a distance of about 5 km from the shoreline. In Eq. (4),  $N$  is the Brunt–Vaisala frequency of the layer above the mixed layer.

We can show that the empirical Eq. (4) is consistent with the simple model (Venkatram, 1977) for the internal boundary height,  $H$ , given by

$$H = \left( \frac{2Q_o(1+A)x}{U\gamma} \right)^{1/2}, \tag{5}$$

where  $Q_o$  is the average kinematic heat flux over land,  $A$  is the ratio of the surface to the inversion

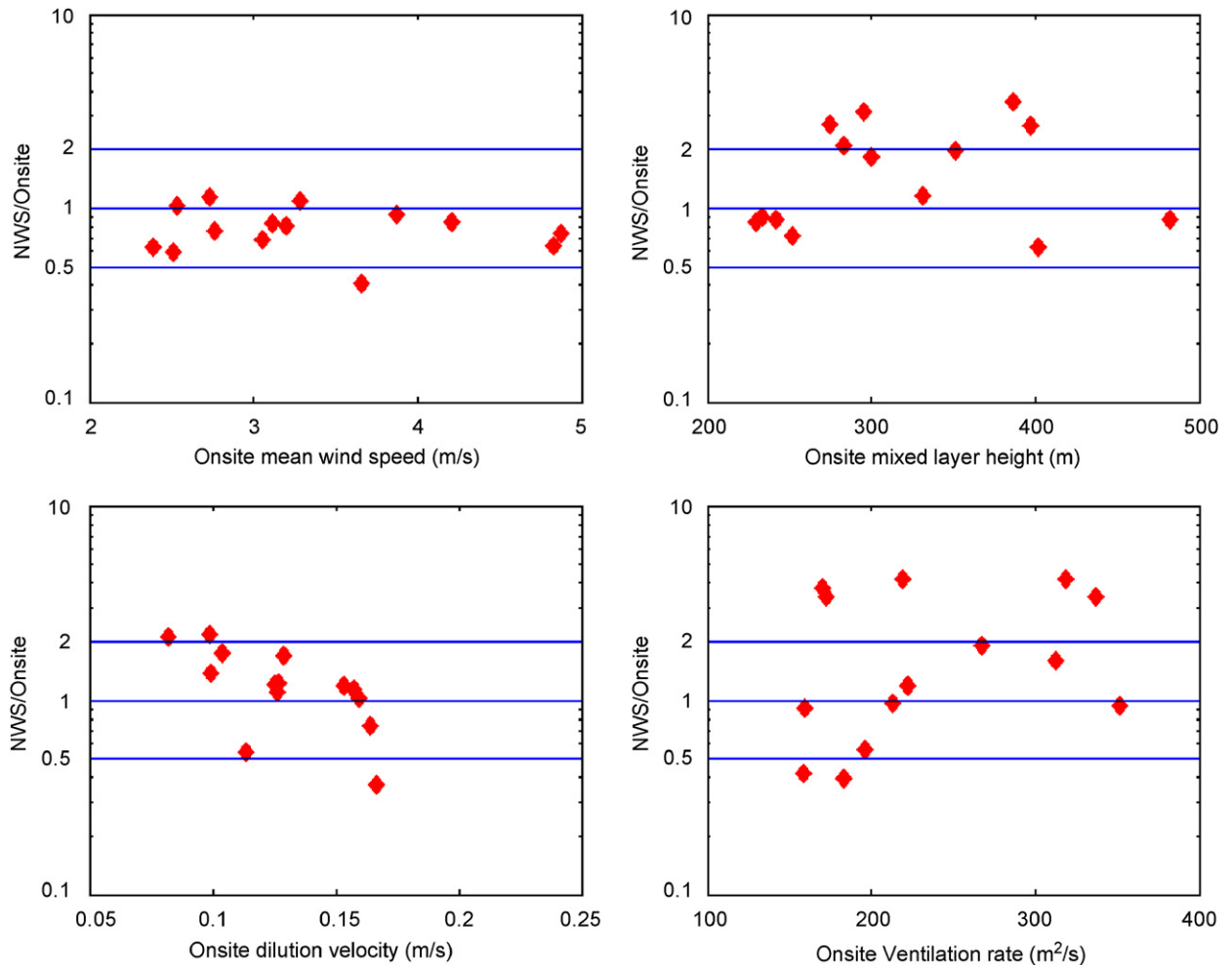


Fig. 5. Comparison of mean winds, mixed layer heights, dilution velocities and ventilation rates estimated using onsite observations with values obtained from NWS data. The horizontal lines above and below the unity line correspond to a factor of two.



heat flux,  $x$  is the distance from the shoreline,  $U$  is boundary layer averaged wind speed, and  $\gamma$  is the potential temperature gradient above the convective internal boundary layer.

If we assume that the measured vertical velocity fluctuations are dominated by convection, we can write

$$\sigma_w = \alpha \left( \frac{g}{T_o} Q_o H \right)^{1/3}, \tag{6}$$

where  $\alpha = 0.6$  (Stull, 1988) and  $T_o$  is a reference temperature whose precise value does not affect the calculations. Substituting Eq. (6) in Eq. (5), and using the definition of the Brunt–Vaisala frequency

$$N = \left( \frac{g}{T_o} \gamma \right)^{1/2}, \tag{7}$$

we find that

$$H = \frac{\sigma_w}{N} \left( \frac{Nx}{U} \right)^{1/3} \frac{(2(1+A))^{1/3}}{\alpha}. \tag{8}$$

Using typical values of  $N$  and  $U$ , and  $A = 0.2$  (Venkatram, 1977) for the Wilmington experiment, we find that the variables within the parenthesis yield a value of about 6.5, which is consistent with the empirically determined value of 8.

When the tracer is well mixed through the boundary layer, the ground-level concentration is inversely proportional to the product of the horizontal plume spread, the mixed layer height, and the mean wind speed. This implies that the concentration is inversely proportional to the product of the standard deviation of the horizontal

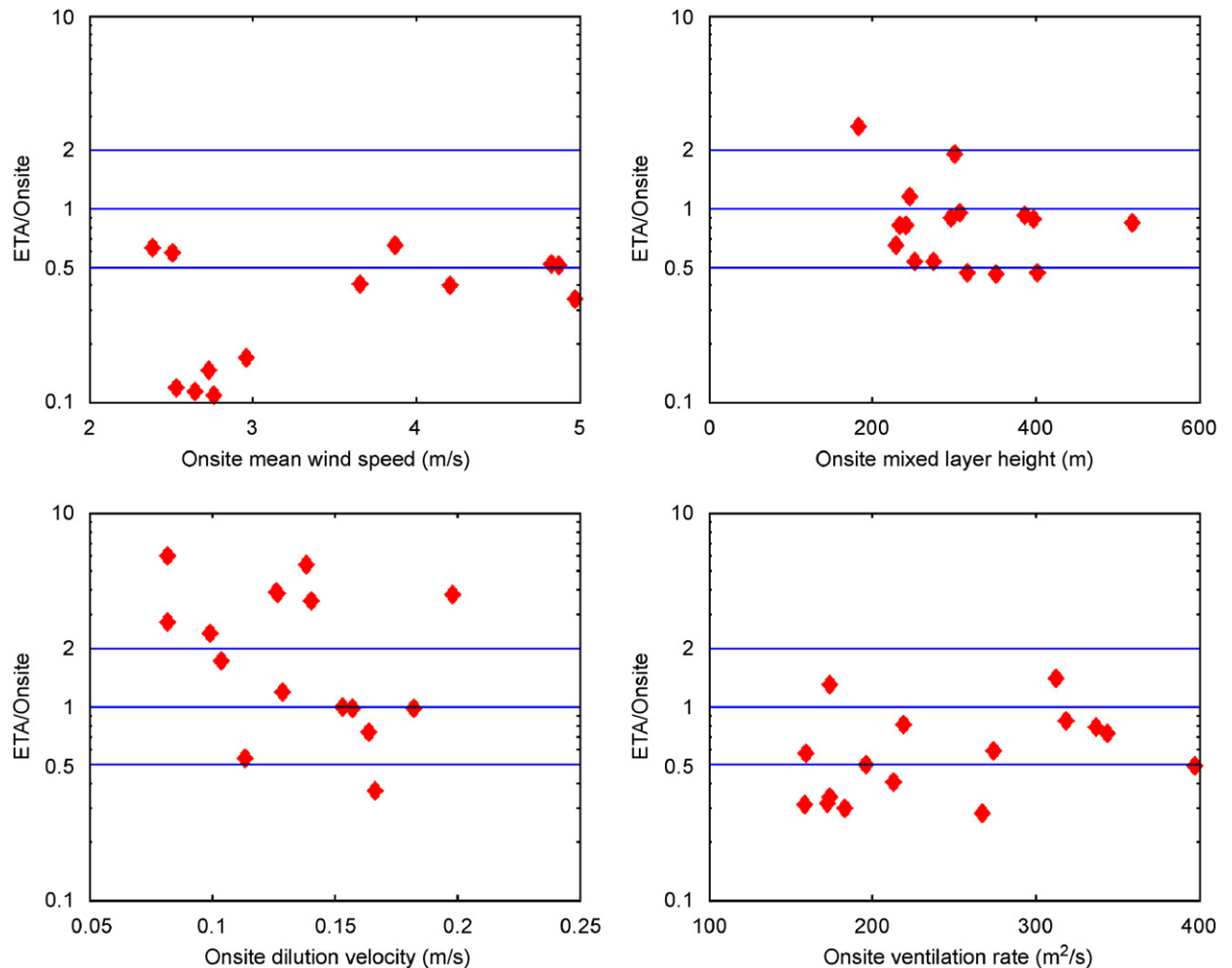


Fig. 6. Comparison of mean winds, mixed layer heights, dilution velocities and ventilation rates estimated using onsite observations with values obtained from ETA output. The horizontal lines above and below the unity line correspond to a factor of two.

velocity fluctuations,  $\sigma_v$ , and mixed layer height,  $H$ . We will refer to  $\sigma_v H$  as the ventilation rate.

The ventilation rate is a function of distance from the shoreline. Here, we will characterize the ventilation rate in terms of the maximum boundary height at 5 km or the value predicted by MM5 and Eta in the grid square that covers Wilmington. For elevated releases, the ground-level concentration is governed by the fraction of the plume that is entrained into the growing internal boundary layer. This fraction depends on buoyant plume rise and buoyancy induced plume spread, both of which are functions of  $N$ , the Brunt–Vaisala frequency. Because the field study considered here includes only surface releases, we do not examine the sensitivity of modeled concentrations to the Brunt–Vaisala frequency.

The dilution velocity determines the near source concentrations for ground-level releases; an over-prediction of the velocity will lead to an under-prediction of concentrations. Underestimation of ventilation rates leads to overestimation of ground-level concentrations.

Fig. 5 compares the mean boundary layer winds, mixed layer heights, dilution velocities and ventilation rates constructed from the NWS data with the corresponding onsite values. The NWS mean winds compare well with the onsite data. The mixed layer heights are overestimated on an average. Most of the estimated dilution velocities are within the factor of two interval. Although there is little bias in the NWS ventilation rates, only about half of them are within a factor of two of the estimated values.

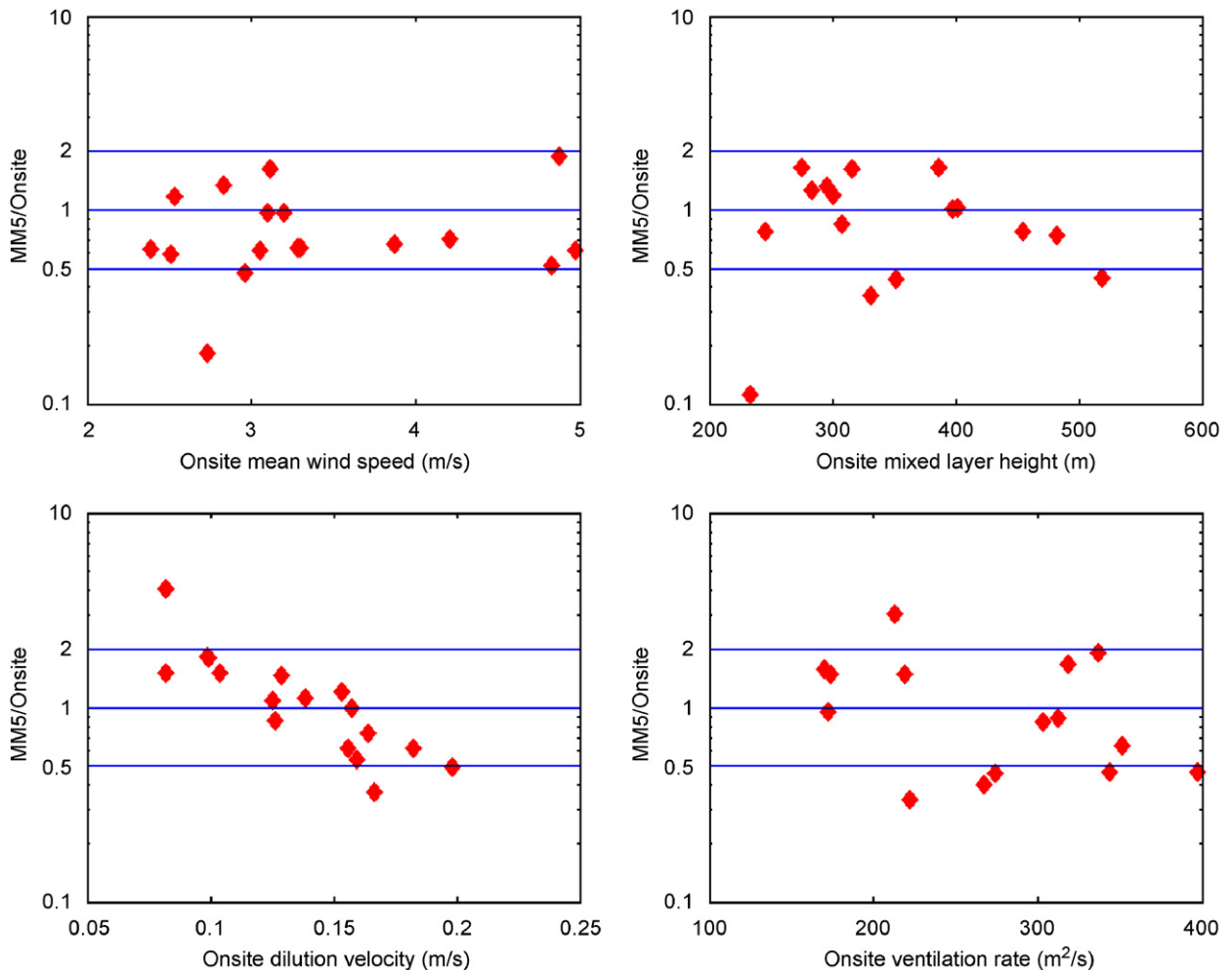


Fig. 7. Comparison of mean winds, mixed layer heights, dilution velocities and ventilation rates estimated using onsite observations with values obtained from MM5 output. The horizontal lines above and below the unity line correspond to a factor of two.

Fig. 6 indicates that Eta underestimates the mean winds by large factors. More than half of the dilution velocities are overestimated by more than a factor two. The same fraction of mixed layer heights is underestimated by a factor of two. The dilution velocities are also underestimated on average.

Fig. 7 shows that meteorological variables derived from MM5 output are generally within a factor of two of the onsite values. But, there are a few mixed layer heights that are severely underestimated.

The next section examines the effects of these discrepancies between modeled values and onsite observations of meteorological variables on estimates of ground-level concentrations corresponding to the Wilmington tracer experiment.

### 5. Modeling tracer concentrations

The study by Yuan et al. (2006) showed that a simple dispersion model that used onsite mean wind and turbulence data as inputs provided an adequate description of the ground-level concentrations observed during the tracer experiment. Because the model has an underlying structure and input requirements similar to those of AERMOD, conclusions related to the sensitivity of its outputs to variations in meteorological inputs should apply to AERMOD and other similar models. We also show later that the model, which we will refer to as the Wilmington Dispersion Model (WDM) for convenience, is an adequate surrogate for AERMOD in explaining the Wilmington data.

Before using WDM to evaluate the usefulness of the outputs from the MM5 and Eta models we describe the essential features of WDM. The ground-level concentration is given by

$$\frac{C(x, y = 0, z = 0)}{Q} = \frac{1}{\pi U \sigma_y \sigma_z} \exp\left(-\frac{h_s^2}{2\sigma_z^2}\right), \quad (9)$$

where  $x$  is the downwind distance from release,  $h_s$  is the release height, and  $U$  is the transport wind speed. The growth rate of the observed horizontal spread,  $\sigma_y$ , is given by

$$\sigma_y = \frac{i_y x}{(1 + x/L_y)^{1/2}}, \quad (10)$$

where  $i_y = \sigma_v/U$  is the horizontal turbulent intensity at a height of 50 m. The length scale,  $L_y$ , was taken to be 2500 m, a value suggested by Briggs (1973) for use in urban areas on the basis of his

analysis of the St. Louis experiment (McElroy and Pooler, 1968).

The vertical spread plume is expressed as

$$\sigma_z = \min\left(\sigma_{z0} + \frac{\sigma_w x}{U} \left(1 + \frac{x}{H}\right)^{1/2}, \sqrt{\frac{2}{\pi}} H\right), \quad (11)$$

where  $H$  is given by Eq. (4) for the onsite model inputs. For MM5, Eta, and NWS data are used,  $H$  is taken to be the boundary layer height in the grid square corresponding to Wilmington. The initial vertical spread,  $\sigma_{z0}$ , is taken to be 32 m to account building induced spread for the experiments during days 1–5 when the tracer was released behind the buildings.

Our analysis indicates that both prognostic models, the Eta Model and MM5, have a limited ability to resolve local wind flow patterns near Wilmington, California with the chosen horizontal resolutions. Therefore, we modeled tracer concentrations assuming that the wind direction is aligned with the centerline of the observed plume.

Fig. 8 compares WDM with AERMOD, using the same meteorological input data from NWS. The results from the two models are within a factor of two, suggesting that WDM can be used as a surrogate for AERMOD in this particular application.

Model performance is described in terms of the statistics of the ratio  $C_p/C_o$ , where  $C_o$  and  $C_p$  refer to the observed and predicted concentrations,

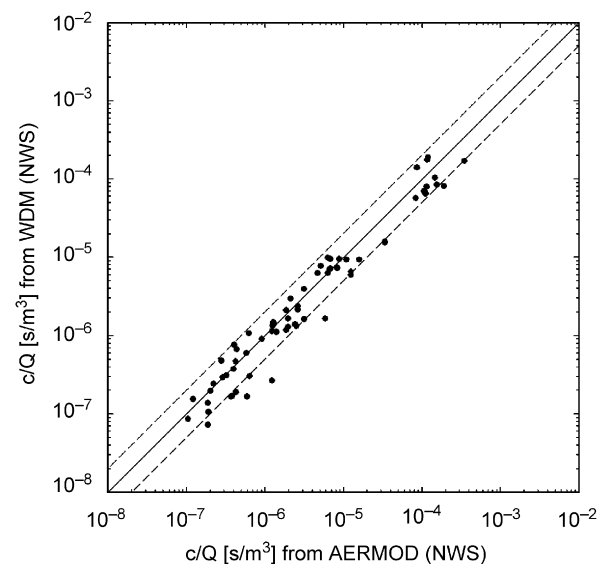


Fig. 8. Comparison between WDM and AERMOD (base case) using NWS data.

respectively. Then, the bias in the model estimate is characterized by  $m_g$ , the geometric mean of the ratio:

$$m_g = \exp(\text{mean}(\varepsilon)),$$

where

$$\varepsilon = \log\left(\frac{C_p}{C_o}\right) \tag{12}$$

and the spread of observations about a model estimate is quantified using the geometric standard deviation,  $s_g$ ,

$$s_g = \exp(\text{standard deviation of } \varepsilon). \tag{13}$$

Then, if the observed concentrations are lognormally distributed about the model estimate, the

95% confidence interval of the ratio of the observed to the estimated concentration is approximately given by the interval  $m_g s_g^{1.96}$  to  $m_g s_g^{-1.96}$ .

Model performance measures defined in Eq. (13) allows for the familiar interpretation of bias: a value of greater than 1 implies that the model is over-estimating, while a value less than unity implies under prediction. The correlation between these arc maximums is quantified by  $r^2$ , which is the fraction of the variance of the logarithm of observed concentrations explained by the model.

Fig. 9 shows a comparison between WDM estimates using onsite data and observed tracer concentrations for two sets of experiments: one corresponding to releases inside the cluster of buildings in the LADWP power plant, and

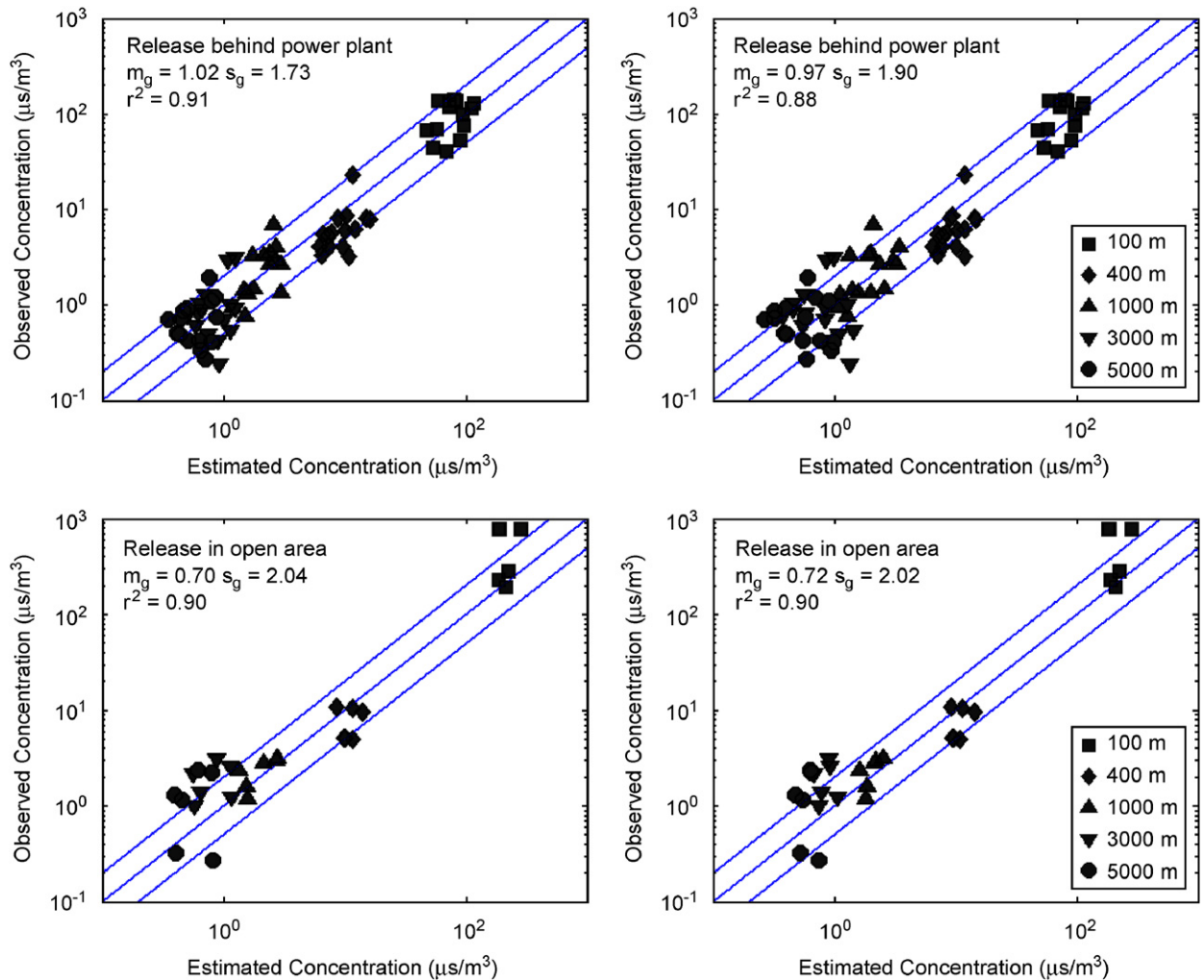


Fig. 9. Performance of WDM using onsite data. Right panels correspond to maximum boundary layer heights calculated using Eq. (14).

the other to releases in an open area close to the power plant. This division was designed to examine the importance of building enhanced plume spread. The first set of releases was conducted during the first 5 days of the experiment, and the second set during the last 2 days. Note that at a receptor distance of 100 m, the concentrations associated with the release from the open area are several times those corresponding to the release behind the power plant. The concentrations are lower for the release behind the power plant because of the initial plume spread induced by the power plant building.

The right panels refer to boundary heights calculated with measured/modeled values of  $\sigma_w$

and a nominal value of  $N = 0.014 \text{ s}^{-1}$ , corresponding to the average of the values observed in the field experiment.

$$H = 8 \frac{\sigma_w}{(N = 0.014 \text{ s}^{-1})} \quad (14)$$

We used Eq. (14) to estimate concentrations to see whether the empirical estimate of  $H$  suggested by the field experiment resulted in improvements in the performance of WDM when the inputs were derived from other sources: NWS, Eta, and MM5. As expected, the use of this equation with onsite data does not result in a noticeable change in model performance, because Eq. (14) was derived from onsite data. We expect the model

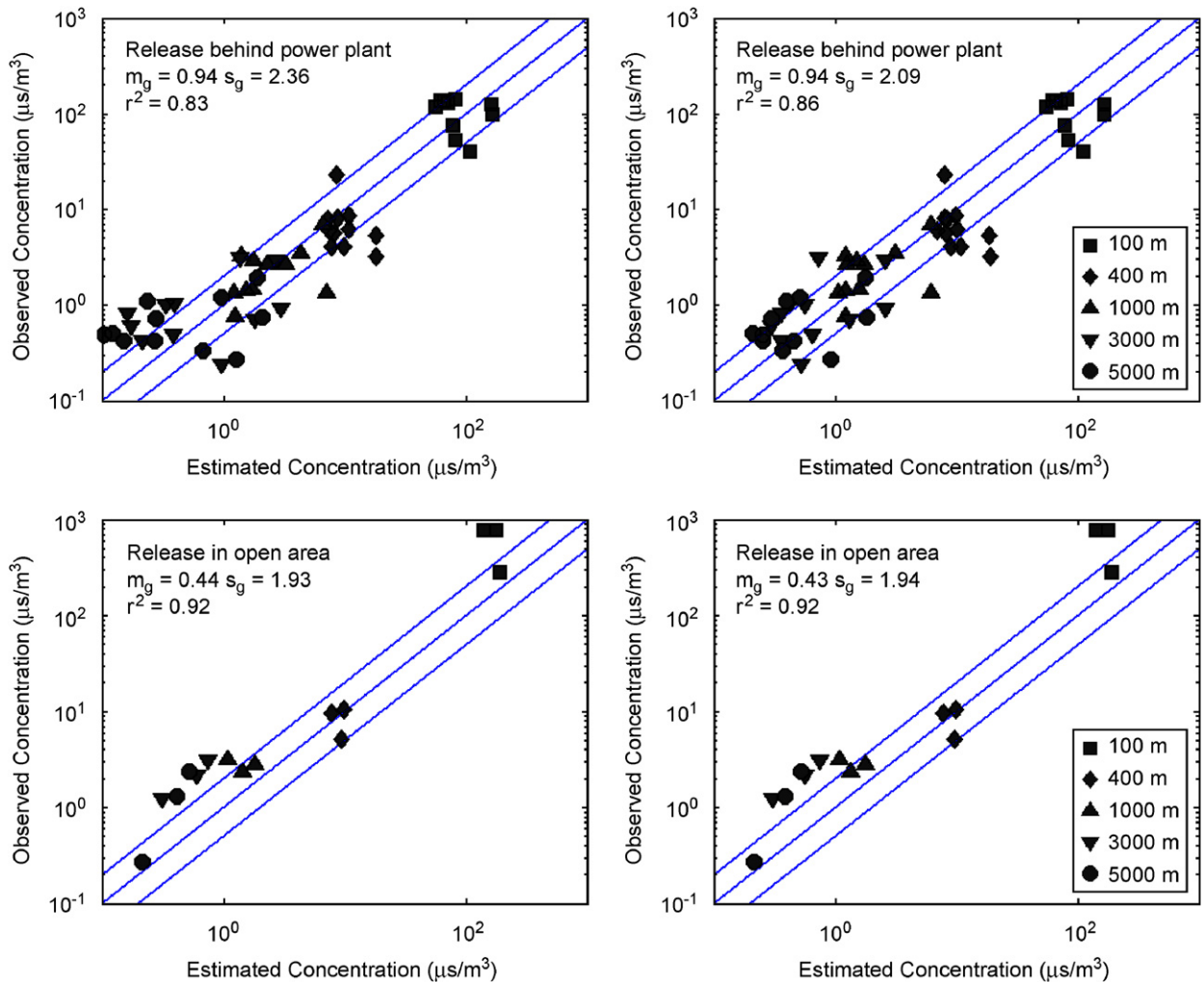


Fig. 10. Same as Fig. 9 except that input data correspond to NWS observations. Right panels correspond to maximum boundary layer heights calculated using Eq. (14).

performance corresponding to the onsite data to set the standard to compare with the performances associated with meteorological inputs from NWS, Eta, and MM5.

Fig. 10 shows the performance of WDM when NWS data is used to construct model inputs. The model performance is not as good as that with onsite data:  $s_g$  increases from 1.73 to 2.36. The concentrations at 3000 and 5000 m are underestimated for the releases behind the power plant suggesting that boundary layer height might be overestimated. Using the empirical equation for the boundary layer does result in the  $s_g$  decreasing from 2.36 to 2.09. The corresponding change for releases in the open area is not noticeable because of the much smaller number of data points.

Fig. 11 shows the performance of WDM when Eta output is used to construct model inputs. The concentrations at all receptor distances beyond 100 m are overestimated because of the underestimation of ventilation rates. The overestimation is reduced when the boundary layer height is estimated with the empirical Eq. (14).

Fig. 12 shows the performance of WDM corresponding to MM5 model inputs. Most of the estimated concentrations are within a factor of two of the observations. A small fraction of the observations are substantially overestimated, corresponding to the underestimated values of values of ventilation rates seen in Fig. 5. This overestimation disappears once the boundary layer height is estimated with Eq. (14).

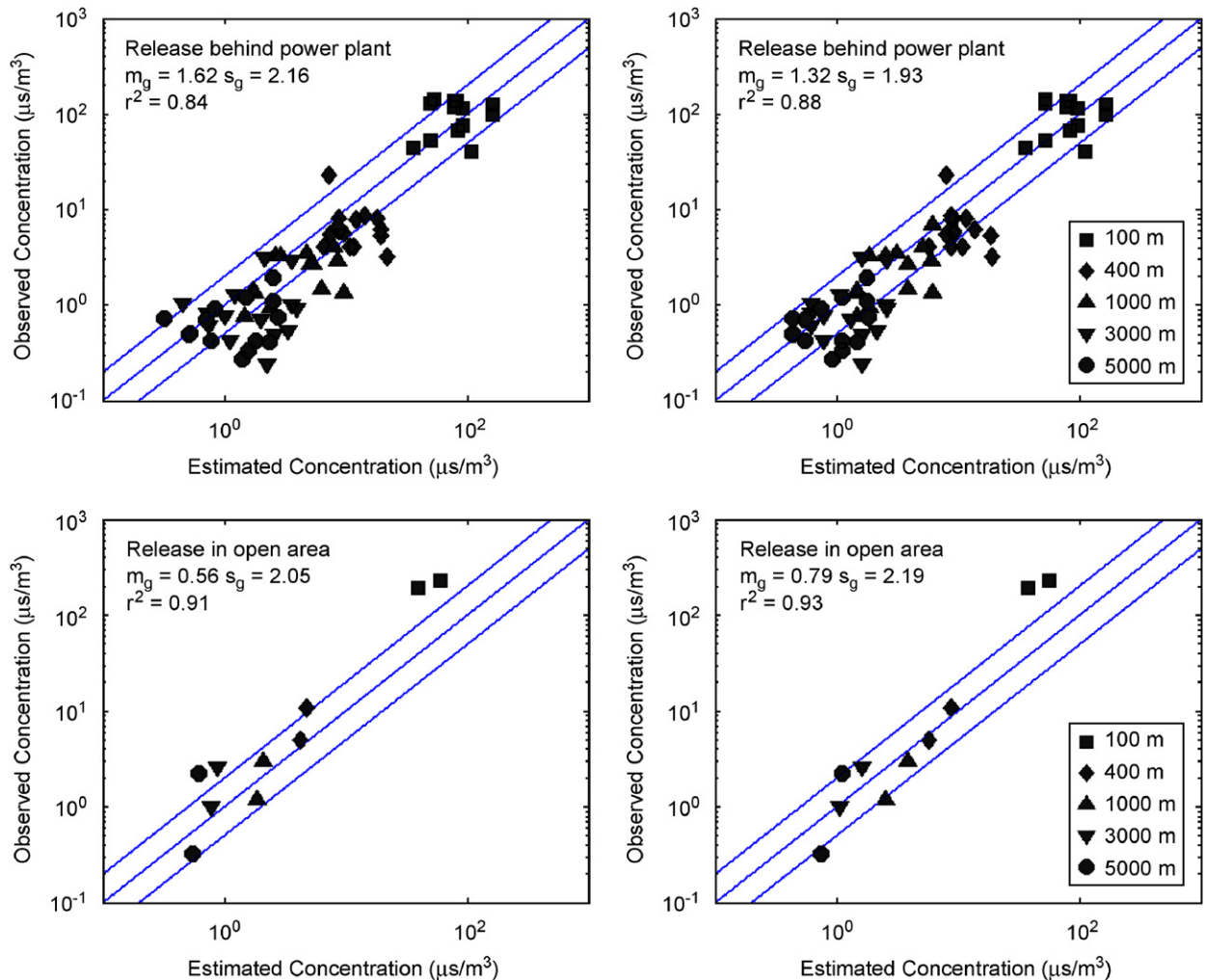


Fig. 11. Same as Fig. 9 except that input data correspond to Eta output. Right panels correspond to maximum boundary layer heights calculated using Eq. (14).

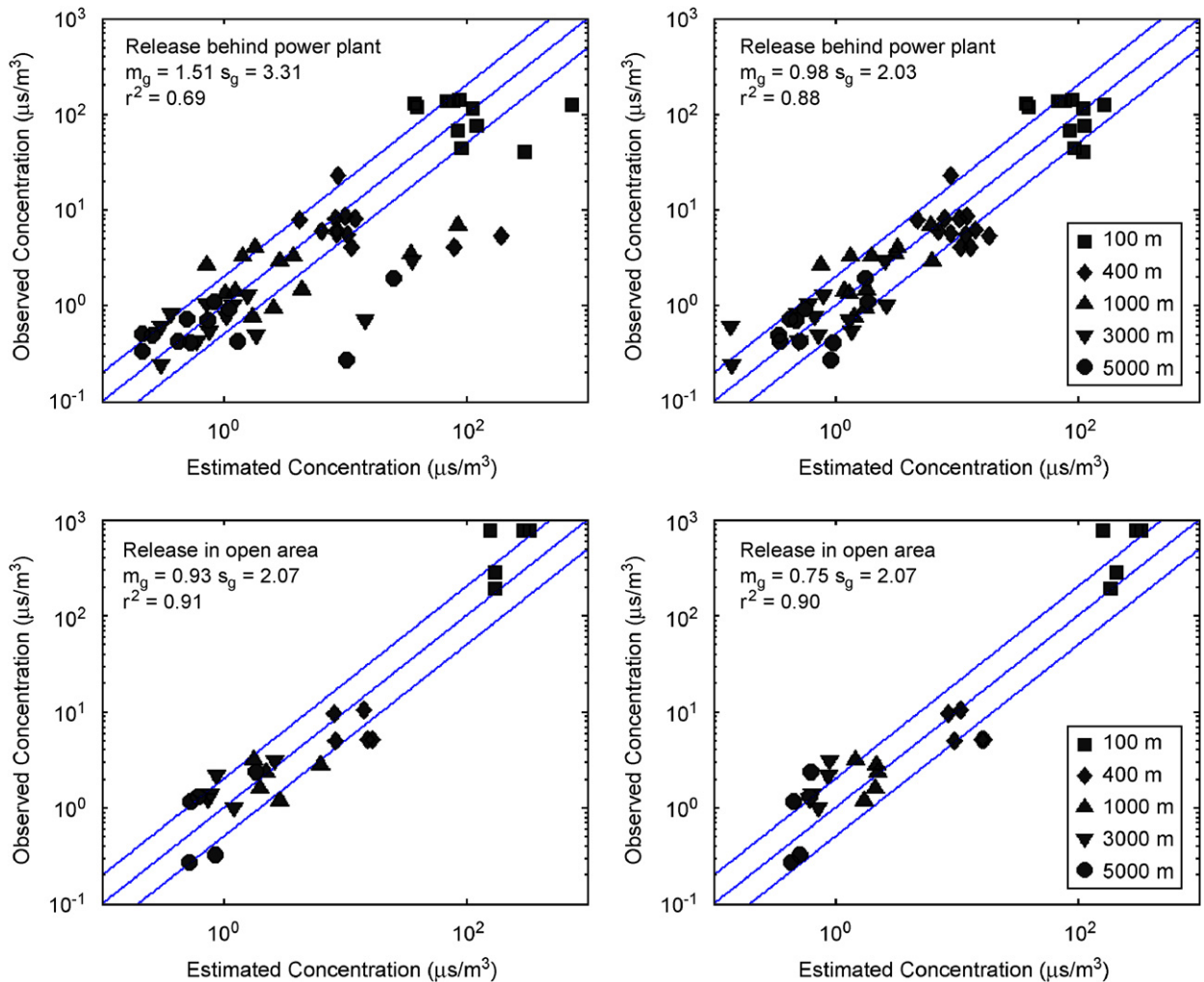


Fig. 12. Same as Fig. 9 except that input data correspond to MM5 output. Right panels correspond to maximum boundary layer heights calculated using Eq. (14).

### 6. Summary

The paper addresses the question: Can outputs from comprehensive prognostic meteorological models, such as MM5 and Eta, replace onsite observations or NWS observations from nearby sites as inputs to dispersion models, such as AERMOD? The results from this study indicate that these meteorological models have difficulty in estimating wind direction at Wilmington, which is a coastal site. But, MM5 with a grid resolution of 3 km performs better than the 12 km resolved Eta model in describing the sea breeze related flow patterns observed at Wilmington. Except for a few cases, MM5 provides adequate estimates of the maximum mixed layer heights observed at the site.

Eta, on the other hand, tends to underestimate mixed layer heights. These results indicate that comprehensive models can simulate mixed layer heights, wind directions and speeds if the model resolution is consistent with the scale of the flow patterns of interest. However, it should be noted that smaller horizontal grid spacing does not guarantee higher accuracy in mesoscale models (cf. Mass et al., 2002).

Prognostic meteorological models routinely provide turbulent kinetic energy (TKE) as an output, which can be used to generate turbulent velocities required by dispersion models, such as AERMOD. This study shows that a dispersion model, similar to AERMOD, using turbulent velocities generated from MM5 and Eta, provides concentration

estimates that compare well with those corresponding to nearby NWS observations or onsite measurements. For the Wilmington, CA, cases shown here, the more highly resolved MM5 performs better than Eta.

It is not clear that these prognostic models can simulate the thermal internal boundary layer (TIBL) that grows with distance from the shoreline; they provide one value for the entire grid square corresponding to the Wilmington experimental site. The spatial details of the TIBL might not be important for the ground-level releases of the field experiment considered in this paper. But the TIBL plays a critical role for elevated releases when ground-level concentrations are controlled by the rate at which the growing TIBL entrains the elevated plume (Misra and Onlock, 1982 for example). Thus, we need to be cautious about using boundary layer heights from a poorly resolved meteorological model for shoreline dispersion applications, or other situations when the spatial variations of surface characteristics are important.

This study shows that meteorological observations from nearby NWS sites can be processed using simple boundary models to provide input variables that are comparable in usefulness to those derived from onsite measurements. In the absence of NWS observations, comprehensive meteorological models, such as MM5 and Eta, have the potential of providing meteorological inputs for dispersion models. Because wind direction estimates from such forecast models may not be reliable in coastal zones and in complex terrain, the value of their other boundary layer outputs can be enhanced by supplementing them with local measurements of wind direction and speed using inexpensive anemometers.

### Acknowledgements

Dr Akula Venkatram's research was supported by the National Science Foundation through grant ATM 0430776.

### Disclaimer

The research presented here was performed under the Memorandum of Understanding between the US Environmental Protection Agency (EPA) and the US Department of Commerce's National Oceanic and Atmospheric Administration (NOAA) and under agreement number DW13921548. This work constitutes a contribution to the NOAA Air Quality Program. Although it has been reviewed by

EPA and NOAA and approved for publication, it does not necessarily reflect their policies or views.

### References

- Black, T., 1994. The new NMC mesoscale eta model: description and forecast examples. *Weather Forecasting* 9, 265–278.
- Briggs, G.A., 1973. Diffusion estimation for small emissions. In ERL, ARL USAEC Report ATDL-106, US Atomic Energy Commission, Oak Ridge, Tennessee.
- Byun, D.W., Ching, J.K.S., (Eds.), 1999. Science algorithms of the EPA Models-3 Community Multiscale Air Quality (CMAQ) Modeling System. US Environmental Protection Agency Rep. EPA-600/R-99/030, 727pp. [Available from Office of Research and Development, EPA, Washington, DC 20460.]
- Byun, D.W., Schere, K., 2006. Review of the governing equations, computational algorithms, and other components of the models-3 community multiscale air quality (CMAQ) modeling system. *Applied Mechanics Review* 59, 51–77.
- Cairns, M.M., Corey, J., 2003. Mesoscale model simulations of high-wind events in the complex terrain of Nevada. *Weather Forecasting* 18, 249–263.
- Chang, J.S., Brost, R.A., Isaken, I.S.A., Madronich, S., Middleton, P., Stockwell, W.R., Walcek, C.J., 1987. A three-dimensional Eulerian acid deposition model: physical concepts and formulation. *Journal of Geophysical Research* 92, 14,681–14,700.
- Cheng, W.Y.Y., Steenburgh, W.J., 2005. Evaluation of surface sensible weather forecasts by the WRF and the eta models over the Western United States. *Weather Forecasting* 20, 812–821.
- Cimorelli, A.J., Perry, S.G., Venkatram, A., Weil, J.C., Paine, R.J., Wilson, R.B., Lee, R.F., Peters, W.D., Brode, R.W., 2005. AERMOD: a dispersion model for industrial source applications. Part I: general model formulation and boundary layer characterization. *Journal of Applied Meteorology* 44, 682–693.
- Desert Research Institute (DRI), 2005. Mesoscale Model 5 (MM5) Real Time Forecasting Results for California. [URL: <http://www.adim.dri.edu/Projects/CalBoat/jsp/index.html>].
- Draxler, R.R., 2003. Evaluation of an ensemble dispersion calculation. *Journal of Applied Meteorology* 42, 308–317.
- Draxler, R.R., Hess, G.D., 1998. An overview of the Hysplit\_4 modeling system for trajectories, dispersion, and deposition. *Australian Meteorology Magazine* 47, 295–308.
- Grell, G.A., Dudhia, J., Stauffer, D.R., 1995. A description of the Fifth-Generation Penn State/NCAR Mesoscale Model (MM5). NCAR Tech. Note. TN-398 + STR, 122pp. [URL: <http://www.mmm.ucar.edu/mm5/doc1.html>].
- Hanna, S.R., Britter, R.E., 2001. Wind Flow and Vapor Cloud Dispersion at Industrial and Urban Sites. AICHE, 3 Park Ave, New York, NY, 10016, 171pp.
- Janjic, Z.I., 1994. The step-mountain eta coordinate model: further developments of the convection, viscous sublayer, and turbulence closure schemes. *Monthly Weather Review* 122, 927–945.
- Koraćin, D., Dorman, C., 2001. Marine atmospheric boundary layer divergence and clouds along California in June 1996. *Monthly Weather Review* 129, 2040–2056.



- Koraćin, D., Dorman, C.E., Dever, E.P., 2004. Coastal perturbations of marine layer winds, wind stress, and wind stress curl along California and Baja California in June 1999. *Journal of Physical Oceanography* 34, 1152–1173.
- Koraćin, D., Businger, J.A., Dorman, C.E., Lewis, J.M., 2005. Formation and evolution, and dissipation of coastal sea fog. *Boundary-Layer Meteorology* 117, 447–478.
- Mass, C.F., Ovens, D., Westrick, K., Colle, B.A., 2002. Does increasing horizontal resolution produce more skillful forecasts? *Bulletin Of the American Meteorology Society* 83, 407–430.
- McElroy, J.L., Pooler, F., 1968. The St. Louis dispersion study—volume II—analysis. National Air Pollution Control Administration, Pub. No. AP-53, US DHEW Arlington, 50 pages.
- Misra, P.K., Onlock, S., 1982. Modelling continuous fumigation of Nanticoke generating station plume. *Atmosphere Environment* 16, 479–489.
- Otte, T.L., Pouliot, G., Pleim, J.E., Young, J.O., Schere, K.L., Wong, D.C., Lee, P.C.S., Tsidulko, M., McQueen, J.T., Davidson, P., Mathur, R., Chuang, H.-Y., DiMego, G., Seaman, N.L., 2005. Linking the eta model with the community multiscale air quality (CMAQ) modeling system to build a national air quality forecasting system. *Weather Forecasting* 20, 367–384.
- Rogers, E., Black, T.L., Deaven, D.G., DiMego, G.J., Zhao, Q., Baldwin, M., Junker, N.W., Lin, Y., 1996. Changes to the operational “early” Eta Analysis/Forecast System at the national centers for environmental prediction. *Weather Forecasting* 11, 391–413.
- Stull, R., 1988. *An Introduction to Boundary Layer Meteorology*. Kluwer Academic Publishers, 684pp.
- Touma, J., Isakov, V., Ching, J., Seigneur, C., 2006. Air quality modeling of hazardous pollutants: current status and FUTURE directions. *Journal of the Air & Waste Management Association* 56, 547–558.
- Venkatram, A., 1977. A model of internal boundary-layer development. *Boundary-Layer Meteorology* 11, 419–437.
- Yamada, T., Bunker, S., Moss, M., 1992. Numerical simulations of atmospheric transport and diffusion over coastal complex terrain. *Journal of Applied Meteorology* 31, 565–578.
- Yuan, J., Venkatram, A., Isakov, V., 2006. Dispersion from ground-level sources in a shoreline urban area. *Atmospheric Environment* 40, 1361–1372.